

# Predicting walking response to ankle exoskeletons using data-driven models

Michael C. Rosenberg<sup>1</sup>, Bora S. Banjanin<sup>2</sup>, Samuel A. Burden<sup>2</sup>, Katherine M. Steele<sup>1</sup>

<sup>1</sup> Department of Mechanical Engineering, University of Washington, Seattle, WA, USA

<sup>2</sup> Department of Electrical and Computer Engineering, University of Washington, Seattle, WA, USA

Correspondence: mcrosenb@uw.edu

## I. KEYWORDS

Ankle exoskeleton; data-driven modeling; locomotion; prediction; joint kinematics; muscle activity

## II. ABSTRACT

Despite recent innovations in exoskeleton design and control, predicting subject-specific impacts of exoskeletons on gait remains challenging. We evaluated the ability of three classes of subject-specific phase-varying models to predict kinematic and myoelectric responses to ankle exoskeletons during walking, without requiring prior knowledge of specific user characteristics. Each model – phase-varying (PV), linear phase-varying (LPV), and nonlinear phase-varying (NPV) – leveraged Floquet Theory to predict deviations from a nominal gait cycle due to exoskeleton torque, though the models differed in complexity and expected prediction accuracy. For twelve unimpaired adults walking with bilateral passive ankle exoskeletons, we predicted kinematics and muscle activity in response to three exoskeleton torque conditions. The LPV model's predictions were more accurate than the PV model when predicting less than 12.5% of a stride in the future and explained 49–70% of the variance in hip, knee, and ankle kinematic responses to torque. The LPV model also predicted kinematic responses with similar accuracy to the more-complex NPV model. Myoelectric responses were challenging to predict with all models, explaining at most 10% of the variance in responses. This work highlights the potential of data-driven phase-varying models to predict complex subject-specific responses to ankle exoskeletons and inform device design and control.

### 26 III. INTRODUCTION

27 Ankle exoskeletons are used to improve kinematics and reduce the energetic demands of locomotion in  
28 unimpaired adults and individuals with neurologic injuries [1-5]. Customizing exoskeleton properties to  
29 improve an individual's gait is challenging and accelerating the iterative experimental process of device  
30 optimization is an active area of research [6, 7]. Studies examining the effects of exoskeleton properties –  
31 sagittal-plane ankle stiffness or equilibrium ankle angle for passive exoskeletons and torque control laws for  
32 powered exoskeletons – on kinematics, motor control, and energetics have developed design and control  
33 principles to reduce the energetic demand of walking and improve the quality of gait [1, 6, 8, 9]. Predicting  
34 how an individual's gait pattern responds to ankle exoskeletons across stance may inform exoskeleton design  
35 by enabling rapid evaluation of exoskeleton properties not tested experimentally. Additionally for powered  
36 exoskeletons, which prescribe torque profiles using feedforward or feedback (e.g. kinematic or myoelectric)  
37 control laws, predicting responses over even 10–20% of a stride may improve tracking performance or  
38 transitions between control modes [4, 10-12]. However, predicting subject-specific responses to exoskeletons  
39 remains challenging for unimpaired individuals and those with motor impairments [2, 12, 13].

40

41 Common physics-based models, including simple mechanical models and more physiologically-detailed  
42 musculoskeletal models, use principles from physics and biology to analyze and predict exoskeleton impacts  
43 on gait. For example, one lower-limb mechanical walking model predicted that an intermediate stiffness in a  
44 passive exoskeleton would minimize the energy required to walk, a finding that was later observed  
45 experimentally in unimpaired adults [1, 14]. More physiologically-detailed musculoskeletal models have  
46 been used to predict the impacts of exoskeleton design on muscle activity during walking in children with  
47 cerebral palsy and running in unimpaired adults [15, 16]. While these studies identified hypothetical  
48 relationships between kinematics and the myoelectric impacts of exoskeleton design parameters, their  
49 predictions were not evaluated against experimental data.

50

51 Challenges to accurately predicting responses to ankle exoskeletons with physics-based models largely stem  
52 from uncertainty in adaptation, musculoskeletal physiology, and motor control, which vary between  
53 individuals and influence response to exoskeletons. While individuals explore different gait patterns to  
54 identify an energetically-optimal gait, exploration does not always occur spontaneously, resulting in sub-  
55 optimal gait patterns for some users [17]. Popular physiologically-detailed models of human gait typically  
56 assume instantaneous and optimal adaptation, which do not reflect how experience and exploration may  
57 influence responses to exoskeletons, possibly reducing the accuracy of predicted responses [18, 19].  
58 Additionally, when specific measurement sets are unavailable for model parameter tuning, population-  
59 average based assumptions about musculoskeletal properties and motor control are required [17, 20-22].  
60 However, musculoskeletal properties and motor control are highly uncertain for individuals with motor  
61 impairments, today's most ubiquitous ankle exoskeleton users [19, 20, 22, 23]. Musculotendon dynamics and  
62 motor complexity are known to explain unintuitive exoskeleton impacts on gait energetics, suggesting that  
63 uncertain musculotendon parameters and motor control may limit the accuracy of predicted changes in gait  
64 with ankle exoskeletons [19, 21, 24]. Predictions of exoskeleton impacts on gait using physiological models,  
65 therefore, require accurate estimates of adaptation, musculotendon parameters, and motor control.

66

67 Conversely, data-driven approaches address uncertainty in user-exoskeleton dynamics by representing the  
68 system entirely from experimental data. For instance, human-in-the-loop optimization provides a model-free  
69 alternative to physics-based prediction of exoskeleton responses by automatically exploring different  
70 exoskeleton torque control strategies for an individual [6, 7]. This experimental approach requires no prior  
71 knowledge about the individual: optimization frameworks identify torque control laws that decrease  
72 metabolic rate relative to baseline for an individual using only respiratory data and exoskeleton torque  
73 measurements. However, experimental approaches to exoskeleton optimization require the optimal design to  
74 be tested, potentially making the search for optimal device parameters time-intensive. Alternatively, machine  
75 learning algorithms, such as the Random Forest Algorithm, have used retrospective gait analysis and clinical

76 exam data to predict changes in joint kinematics in response to different ankle-foot orthosis designs in  
77 children with cerebral palsy [8]. This study reported good classification accuracy, though predictions may  
78 not generalize to new orthosis designs. Unlike physiologically-detailed or physics-based models, human-in-  
79 the-loop optimization and many machine learning models are challenging to interpret, limiting insight into  
80 how a specific individual's physiology influences response to exoskeleton torque. A balance between  
81 physiologically-detailed and model-free or black-box data-driven approaches may facilitate the prediction  
82 and analysis of responses to ankle exoskeletons without requiring extensive knowledge of an individual's  
83 physiology.

84

85 In this work, we investigated a subject-specific data-driven modeling framework – phase-varying models –  
86 that may fill the gap between physiologically-detailed model-based and model-free experimental approaches  
87 for predicting gait with exoskeletons. Phase-varying models typically have linear structure whose parameters  
88 are estimated from data, enabling both prediction and analysis of gait with exoskeletons [25, 26]. Unlike  
89 physiologically-detailed models, phase-varying models do not require knowledge of the physics or control  
90 of the underlying system. Unlike experimental approaches, the model-based framework enables prediction  
91 of responses to untested exoskeleton designs or control laws.

92

93 Phase-varying models leverage dynamical properties of stable gaits derived from Floquet Theory, which  
94 ensures that the convergence of a perturbed trajectory to a stable limit cycle may be locally approximated  
95 using time-varying linear maps [27]. Similar principles have been shown to generalize to limit cycles in non-  
96 smooth or hybrid systems, such as human walking [28]. Moreover, phase-varying modeling principles have  
97 been applied to biological systems, identifying linear phase-varying dynamics to investigate gait stability and  
98 predict changes in kinematics in response to perturbations [25, 26, 29-31]. Responses to ankle exoskeleton  
99 torques may be similarly defined as perturbations off an unperturbed (*i.e.* zero torque) gait cycle, suggesting  
100 that the principles of phase-varying models will generalize to walking with exoskeletons. To the best of our

101 knowledge, phase-varying models have never been used to study walking with exoskeletons and the extent  
102 to which the principles underlying phase-varying models of locomotion generalize to walking with  
103 exoskeletons is unknown.

104

105 To determine if phase-varying models represent useful predictive tools for locomotion with exoskeletons, the  
106 purpose of this research was to evaluate the ability of subject-specific phase-varying models to predict  
107 kinematic and myoelectric responses to ankle exoskeleton torque during walking. We predicted responses to  
108 exoskeletons in unimpaired adults walking with passive ankle exoskeletons under multiple dorsiflexion  
109 stiffness conditions. We focused on three related classes of phase-varying models with different structures,  
110 complexity, and expected prediction accuracies: a phase-varying (PV), a linear phase-varying (LPV), and a  
111 nonlinear phase-varying (NPV) model. Since passive exoskeletons typically elicit small changes in joint  
112 kinematics and muscle activity, we expected the validity of Floquet Theory for human gait to extend to gait  
113 with exoskeletons, indicating that the LPV model should accurately predict responses to passive exoskeleton  
114 torque [1, 25-27, 29]. We, therefore, hypothesized that the LPV models would predict kinematic and  
115 myoelectric responses to torque more accurately than the PV model and as accurately as the NPV model. To  
116 exemplify the potential utility of subject-specific phase-varying models in gait analysis with ankle  
117 exoskeletons, we show how varying the length of model prediction time horizon may inform measurement  
118 selection for exoskeleton design and control. To assess the viability of data-driven phase-varying models in  
119 gait analysis settings, we evaluated the effect of limiting the size of the training dataset on prediction  
120 accuracy.

121

## 122 IV. METHODS

### 123 A. *Experimental protocol*

124 We collected kinematic and electromyographic (EMG) data from 12 unimpaired adults (6 female / 6 male;  
125 age =  $23.9 \pm 1.8$  years; height =  $1.69 \pm 0.10$  m; mass =  $66.5 \pm 11.7$  kg) during treadmill walking with bilateral

126 passive ankle exoskeletons at a self-selected speed. Each participant performed two sessions on separate days  
127 within a one week span. In the first session, we modified the exoskeletons for fit and comfort and performed  
128 a 20-minute practice session. *Additional detail regarding experimental setup, input variable calculations,*  
129 *modeling algorithms, and statistical analyses can be found in Supplemental – S1.*

130

131 Data were collected during the second session. We monitored changes in kinematics using a modified Helen-  
132 Hayes marker set [32] and a 10-camera motion capture system (Qualisys AB, Gothenburg, SE), and measured  
133 muscle activity using 14 wireless EMG sensors (Delsys Inc., Natick, USA). The EMG sensors were placed  
134 bilaterally on the soleus, medial gastrocnemius, tibialis anterior, vastus medialis, rectus femoris, lateral  
135 hamstrings, and gluteus medius following SENIAM guidelines [33]. Participants performed four randomized  
136 trials on a split-belt instrumented treadmill (Bertec Corp., Columbus, USA) under different exoskeleton  
137 conditions (Fig. 1). Unlike many clinical exoskeletons (ankle-foot orthoses), whose torque profiles are  
138 smooth functions of ankle angle, the passive exoskeletons used in this study generated ankle plantarflexion  
139 torques as a piecewise-linear function of the user's ankle angle, and the exoskeleton's neutral angle and  
140 rotational stiffness. The exoskeletons did not resist plantarflexion, similar to other experimental devices [1,  
141 3]. The four exoskeleton conditions were set to sagittal-plane stiffness values:  $K_0$  (0 Nm/deg),  $K_1$  (1.17  
142 Nm/deg),  $K_2$  (3.26 Nm/deg), and  $K_3$  (5.08 Nm/deg), a range known to alter kinematics and myoelectric  
143 signals during gait (Fig. 1) [1]. Participants walked for six minutes per trial, the last four of which were  
144 recorded, and could rest between trials.

145

146

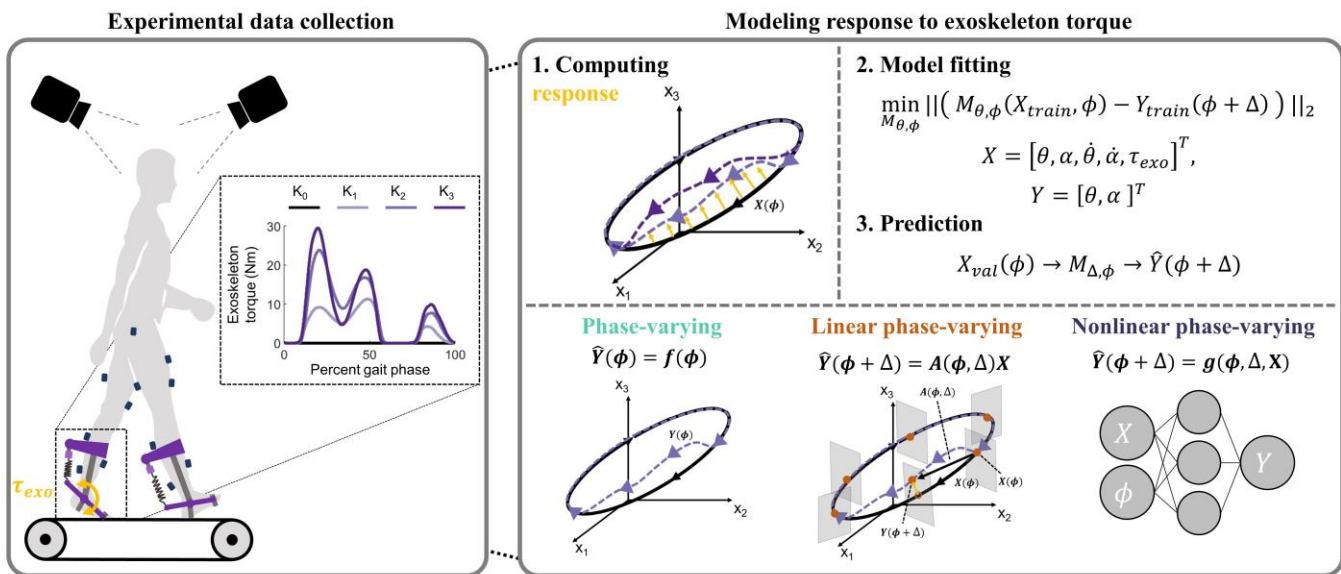


**Fig. 1. Left box:** Data were collected during treadmill walking with bilateral ankle exoskeletons that used linear springs to resist dorsiflexion. Increasing exoskeleton stiffness ( $K_0$ – $K_3$ ) increased exoskeleton torque ( $\tau_{exo}$ , yellow). **Right box:** (1) Purple dashed arrows represent responses to exoskeleton torque, which were defined as deviations from the average zero-torque gait cycle ( $K_0$ ). (2) Response data from the training set were used to fit each model. Input variables included joint kinematics, muscle activity, their time derivatives, and exoskeleton torque. (3): Models were validated by predicting responses from the held-out torque condition using the models fit in (2). **Right box (bottom):** The three phase-varying models were fit and evaluated on the same training and validation sets.

$M_{\Delta,\phi}$  = generic model function of prediction horizon and phase;  $X$  = experimental inputs;  $Y$  = experimental outputs;  $\hat{Y}$  = predicted outputs;  $\phi$  = phase;  $\Delta$  = prediction horizon;  $A$  = linear function;  $f, g$  = nonlinear functions;  $\theta$  = joint kinematics;  $\alpha$  = muscle activation;  $\tau_{exo}$  = exoskeleton torque.

147

148 The marker trajectories were low-pass filtered at 6 Hz using a zero-lag fourth-order Butterworth filter [5].

149 We computed joint kinematics by scaling a generic 29 degree-of-freedom skeletal model to each participant's

150 skeletal geometry and body mass using the inverse kinematics algorithm in OpenSim 3.3 to convert marker

151 trajectories into joint kinematics [18, 34]. To compute linear EMG envelopes, we high-pass filtered the EMG

152 data at 40 Hz, rectified the data, and low-pass filtered at 10 Hz [9]. Kinematic and EMG data were pre-

153 processed using custom scripts in MATLAB (MathWorks, Natick, USA).

154

### 155 B. Gait phase and phase-varying models

156 Unlike the typical gait cycle definition – the percentage of time between successive foot contact events – we

157 used a gait phase based on kinematic posture, which we expected to improve predictions of a system's

158 response to perturbations from the exoskeletons [35]. Using a posture-based gait phase groups kinematically-

159 similar measurements at a specific phase, reducing variance in the data at any point in the cycle, and ensuring  
160 that similar postures across exoskeleton conditions were used during model fitting and prediction. Moreover,  
161 Floquet Theory ensures that phase is well-defined using any periodically-varying measurements [27]. We  
162 used the *Phaser* algorithm, which estimates a system's phase using arbitrary input signals considered to be  
163 phase-locked, to generate gait phase estimates as a function of left and right leg hip flexion angles, similar to  
164 a phase variable proposed to control robotic prostheses [30, 35]. Following gait phase estimation, we modeled  
165 gait using three subject-specific models of response to exoskeletons:

166

167 *1) Phase-varying model*

168 The phase-varying (PV) model was our simplest model and predicts outputs purely as a function of gait  
169 phase. Rather than taking exoskeleton torque as an input, PV model predictions are similar to guessing the  
170 average of the training data at a certain gait phase (Table I) [30, 36]. The PV model takes a phase estimate  
171 as an input and returns a prediction of the system's outputs,  $\hat{Y}_\phi \in \mathbb{R}^M$ , where  $M$  is the number of outputs. The  
172 PV model was parameterized using a seventh-order Fourier Series as a function of phase and served as a  
173 lower bound on prediction accuracy.

174

175 *2) Linear phase-varying model*

176 The linear phase-varying (LPV) model is a discrete-time model that predicts system outputs at a future phase  
177 based on measurements at an initial phase (Table I). For any phase,  $\phi$ , from 0-100% of a stride and a  
178 prediction horizon,  $\Delta$ , the LPV model estimates a map  $A_{\phi,\Delta} \in \mathbb{R}^{M \times N+1}$ , from the initial phase to the final  
179 phase, where  $N + 1$  denotes the number of input variables ( $N$ ) plus a constant term. At 64 initial phases  
180 spaced equally over the gait cycle, we fit discrete maps between initial and final phases using weighted least-  
181 squares regression [25, 26, 29]. We weighted each observation based on the proximity of its phase estimate  
182 to the prescribed initial phase using a Gaussian weighting scheme. For each prediction horizon, the LPV



183 model was represented as a continuously phase-varying function,  $F_{LPV,\Delta}(\phi) \approx A_{\phi,\Delta}$ , parametrized by a  
 184 Fourier Series. We expected the LPV model’s prediction accuracy to exceed that of the PV model [27].

185

186 *3) Nonlinear phase-varying model*

187 While the LPV model should approximate nonlinearities in the dynamics of response to torque, we selected  
 188 a nonlinear phase-varying (NPV) model that serves as an upper bound on prediction accuracy. Specifically,  
 189 we used a three-layer feedforward neural network – a universal function approximator (Table I) [37]. Neural  
 190 networks are considered state-of-the-art predictors and are used in numerous domains, including image  
 191 recognition and robotics [38]. The NPV model’s parameters were tuned for each prediction horizon and  
 192 included phase as an input. We expected the NPV model’s prediction accuracy to meet or exceed that of the  
 193 LPV model.

194

195 Table I: Summary of model structures and expected prediction accuracies.

Model	Functional form	Linear terms	Nonlinear terms	Expected prediction accuracy
Phase-varying (PV)	$\hat{Y}_\phi = F_{PV}(\phi)$	None	Phase	Low
Linear phase-varying (LPV)	$\hat{Y}_{\phi+\Delta} = F_{LPV,\Delta}(\phi)X_\phi$	Inputs	Phase	Moderate
Nonlinear phase-varying (NPV)	$\hat{Y}_{\phi+\Delta} = G_{NPV,\Delta}(\phi, X_\phi)$	None	Phase Inputs	Moderate-High

$F$  = model functions parameterized by a Fourier Series;  $G$  = feedforward neural network model;  $\phi$  = phase;  $\Delta$  = prediction horizon;  $X$  = inputs;  $\hat{Y}$  = predicted outputs

196

197 *C. Inputs and output variables*

198 To reflect clinically-relevant measurements and the dynamics of the neuromusculoskeletal system, we  
 199 selected input variables expected to encode musculoskeletal dynamics and motor control: 3D pelvis  
 200 orientation and lower-limb and lumbar joint angles, processed EMG signals, and their time derivatives at an  
 201 initial phase,  $\phi$  [1, 2, 39]. We appended ten time-history exoskeleton torque samples per leg – uniformly  
 202 distributed between the initial and final phases – to the inputs, resulting in  $N = 80$  inputs [6, 12]. Our decision

203 to use exoskeleton torque samples was motivated by Floquet Theory, according to which an individual's  
204 posture at a future time is a linear function of their initial posture and the exoskeleton torque signal between  
205 initial and final times [27]. Model outputs ( $M = 20$ ) included right and left leg sagittal-plane hip, knee and  
206 ankle kinematics, and EMG signals from each muscle at a future phase,  $\phi + \Delta$ , offset from the initial phase  
207 by prediction horizon  $\Delta$ . While phase-varying models may also predict joint moments, we omitted prediction  
208 of kinetic outcomes due to the presence of sporadic poor force plate strikes for some gait cycles in our dataset.  
209 We modeled response to exoskeleton torque as the deviation from the unperturbed gait cycle (*i.e.* the zero-  
210 torque,  $K_0$  condition) by subtracting the phase-averaged zero-torque gait cycle from each exoskeleton  
211 condition [26, 29]. All data were de-meant and scaled to unit variance of the training set. *Additional detail*  
212 *regarding the selection of torque as model inputs and experimental ground reaction forces can be found in*  
213 *Supplemental – S2.*

214

215 We first computed each model's ability to predict responses to torque within the range of exoskeleton  
216 stiffness levels used to train the models (interpolation) by training each model using the  $K_0$ ,  $K_1$  and  $K_3$   
217 datasets and validating by predicting outputs from the held-out  $K_2$  dataset using inputs from the same dataset  
218 at an initial gait phase. While “what-if” predictions – predicting responses to “untested” (held-out) torques  
219 using nominal kinematics and EMG from a “tested” condition (e.g.  $K_0$ ) – are needed to for predictions to  
220 inform passive exoskeleton design, we chose to predict using the held-out inputs to provide unambiguous  
221 interpretation of each model's prediction accuracy. In “what-if” predictions, errors stem from both poor  
222 model fit and poor matches between the “tested” and “untested” input data at the initial phase. By instead  
223 predicting using “untested” inputs, our predictions errors reflect only the models' fits to each participant's  
224 dynamics and provide upper bounds on the potential accuracy of “what-if” predictions. We selected the  $K_2$   
225 condition for validation in our experimental design because responses in this intermediate torque condition  
226 should be encoded by the  $K_0$ ,  $K_1$ , and  $K_3$  conditions. During validation, experimental outputs from the  $K_2$   
227 condition were compared to the corresponding model predictions.

228

229 We quantified each model's prediction accuracy using the relative remaining variance (RRV) of model  
230 predictions compared to the held-out experimental data [25]. The RRV is calculated as the ratio of the  
231 variances of the prediction error and the experimental data. An RRV value of zero implies a perfect  
232 prediction, while unity RRV values can be achieved by predicting the mean of the validation data. Since we  
233 de-meant the data and predicted deviations from the zero-torque condition, RRV values below unity  
234 indicate that predictions are more accurate than guessing constant (e.g. zero) response to exoskeleton torque.  
235 We computed RRV values for each output using a bootstrapping procedure with 200 iterations [25]. We  
236 computed RRV values for each model over the entire validation time series of approximately 240 strides.  
237 During analysis, the right and left leg RRV values for each output variable were averaged, as we expected  
238 nearly symmetric responses from our unimpaired participants.

239

240 We evaluated the LPV and NPV models' prediction accuracies for the K<sub>2</sub> condition over a range of prediction  
241 horizons, in increments of 6.25% (1/16<sup>th</sup> of a stride), between 6.25 and 100% of a gait cycle. When optimizing  
242 exoskeleton torque profiles, predicting responses using measurements at an initial phase (e.g. initial contact  
243 of the foot with the ground) to achieve a desired outcome at some final phase may be of interest, such as  
244 improving midstance knee kinematics in children with cerebral palsy [2, 3]. However, as the prediction  
245 horizon increases, coherence between measurements at initial and final phases decreases due to nonlinearities  
246 in musculoskeletal dynamics, resulting in prediction accuracies reducing to those of the average prediction  
247 (*i.e.* the PV model), rather than a stride-specific prediction [39-41]. Identifying the maximum prediction  
248 horizon at which initial measurements improve predictions at a final phase may inform exoskeleton control  
249 laws or design criteria. Therefore, we identified the largest prediction horizon lengths at which RRV values  
250 were significantly less than those of the PV model, which were constant across prediction horizons.

251

252 The amount of data required to accurately predict response to exoskeletons will restrict the settings in which  
253 phase-varying models are practical, such as in clinical gait analysis where datasets typically contain only a  
254 few gait cycles [2, 8]. We quantified the impact of training set size on prediction accuracy by determining  
255 the amount of training data needed for prediction accuracies of the  $K_2$  condition to approach to their values  
256 when models were fit using the entire training set ( $RRV_{full}$ ). We iteratively reduced the training set size by  
257 10% of the full size (approximately 24 strides per exoskeleton condition), removing data from the end of  
258 each torque condition in the training set, providing a range of 24-240 strides of training data per condition.  
259 For all training set sizes, we evaluated models using the full-length validation set.

260  
261 To test each model's generalizability across a range of exoskeleton torque conditions, we separately predicted  
262 responses to torque in the  $K_1$ ,  $K_2$ , and  $K_3$  datasets, termed *held-out conditions*, at a 12.5% stride prediction  
263 horizon ( $1/8^{\text{th}}$  of a stride). Predictions over these conditions evaluated both the models' ability to interpolate  
264 ( $K_1$  and  $K_2$ ) and extrapolate ( $K_3$ ) responses to exoskeleton torques included in the training set. For each held-  
265 out condition ( $K_1$ ,  $K_2$ , or  $K_3$ ), we trained the models using kinematic, EMG, and exoskeleton torque inputs  
266 from the zero-torque ( $K_0$ ) condition and the two non-zero-torque exoskeleton conditions not held out for  
267 validation. We evaluated each model by predicting output variables from the held-out exoskeleton condition  
268 using input data at an initial gait phase in the same condition. We compared prediction accuracies across  
269 held-out conditions.

270  
271 To compare differences in performance across the three models, we identified differences in the models'  
272 prediction accuracies using repeated-measures analysis of variance tests at a significance level of  $\alpha = 0.05$ .  
273 When significant differences between models emerged, we identified pair-wise differences between models  
274 using post-hoc paired t-tests ( $\alpha = 0.05$ ) and a Holm-Sidak step-down correction for multiple comparisons [9,  
275 42]. We report percent reductions in RRV values compared to the PV model and percent differences between  
276 the LPV and NPV models.

277

278 V. RESULTS

279 The ankle exoskeletons had the largest impact on ankle kinematics, smaller impacts on knee and hip  
 280 kinematics, and variable impacts on muscle activity (Fig. 2). Compared to the  $K_0$  condition, the peak ankle  
 281 dorsiflexion angle during single-limb support decreased significantly in the  $K_2$  (36.7%) and  $K_3$  (40.0%)  
 282 conditions ( $p < 0.020$ ). Average integrated EMG increased slightly, but not significantly in the hamstrings  
 283 and tibialis anterior ( $p > 0.066$ ) in the  $K_2$  and  $K_3$  conditions compared to the  $K_0$  condition.

284

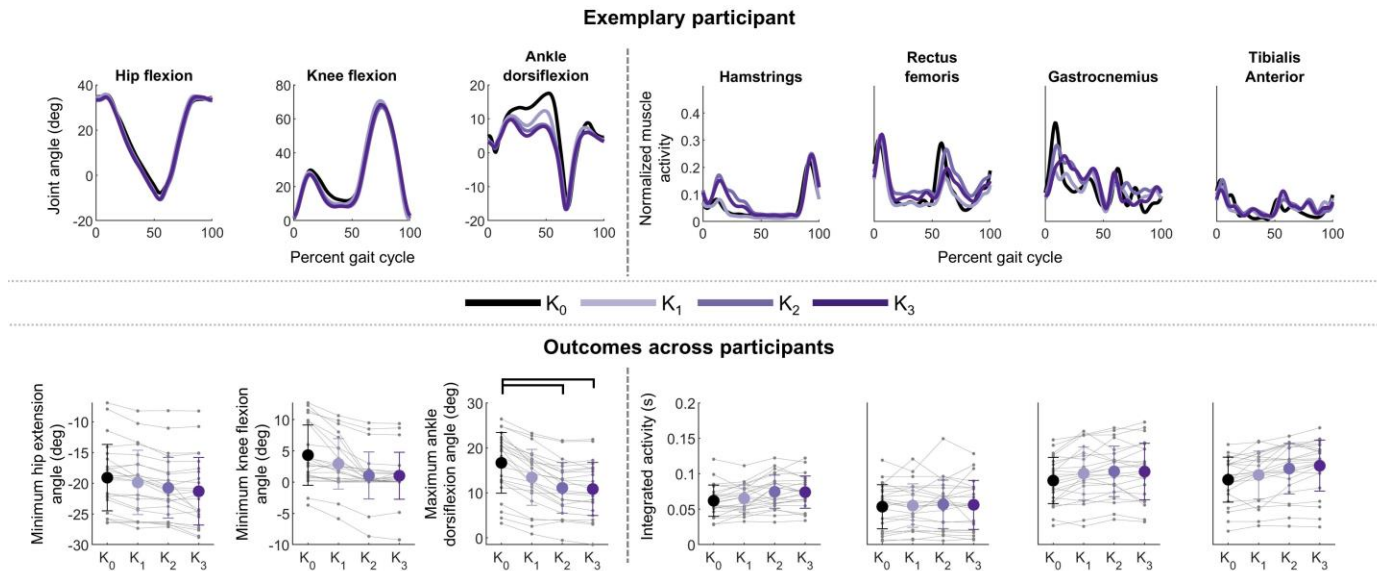


**Fig. 2. Top: Average kinematic (left) and EMG (right) data for one participant who exhibited large, repeatable responses to exoskeleton torque and high model prediction accuracies (P03). Black lines show the zero-torque condition ( $K_0$ ) that was subtracted from all conditions to reflect responses to exoskeleton torque. Bottom: Average ( $\pm 1SD$ ) kinematic and myoelectric responses for all participants in each torque condition. Brackets denote significant differences between exoskeleton conditions according to post-hoc paired t-tests ( $\alpha = 0.05$ ) and a Holm-Sidak step-down correction. Thin gray lines represent individual legs.**

285

286

287 When validating on the held-out  $K_2$  condition, all three models predicted kinematic but not myoelectric  
 288 responses to exoskeleton torque (Fig. 3, dashed lines). At a prediction horizon of  $\Delta = 12.5\%$  of a stride, the  
 289 LPV model's prediction accuracy at the ankle – where the largest responses to torque were observed – was  
 290  $41.6 \pm 16.0\%$  more accurate than the PV model ( $p < 0.001$ ) but not the NPV model ( $p = 0.130$ ; Fig. 4;

291

292 Table II). Similarly, the LPV model's prediction accuracy at the hip was  $41.7 \pm 12.7\%$  better than the PV  
 293 model ( $p < 0.001$ ). However, as prediction horizon increased, the average LPV and NPV model prediction  
 294 accuracies of all outputs except the ankle approached those of the PV model. Changes in knee and hip  
 295 kinematics were predicted more accurately than the baseline PV model for prediction horizons shorter than  
 296  $\Delta = 18.75\%$  of a stride ( $p < 0.001$ ) in the LPV model and  $\Delta = 12.5\%$  of a stride ( $p < 0.001$ ) in the NPV model  
 297 (Fig. 5). At the ankle, the LPV model predicted kinematics 29.1–60.0% more accurately than the PV model  
 298 for all prediction horizons ( $p < 0.001$ ). The NPV model's predictions were significantly more accurate than  
 299 those of the PV model for all prediction horizons except 25.0% and 75.5–81.3% of a stride ( $p < 0.001$ ).

300

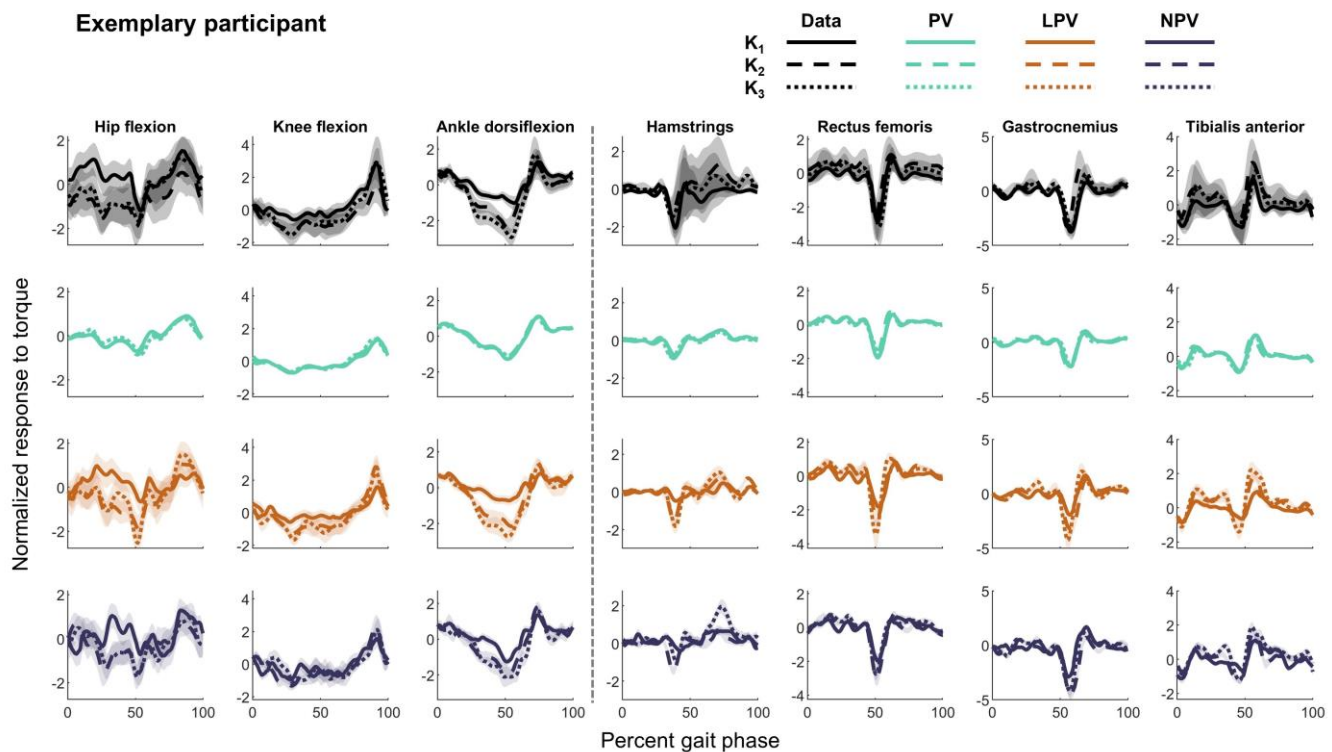


**Fig. 3. Kinematic and myoelectric experimental (black) and predicted (colors) responses to torque for one participant who exhibited large responses to the exoskeletons (P03). Predictions are shown for a prediction horizon of 12.5% of a stride for the PV (green), LPV (orange), and NPV (purple) models. The three held-out conditions are denoted with solid ( $K_1$ ), dashed ( $K_2$ ), and dotted ( $K_3$ ) lines. Lines represent the average ( $\pm 1SD$ ; shaded region) data and predictions over all gait cycles in the corresponding validation dataset. The experimental data show that the  $K_2$  and  $K_3$  responses to torque were more similar to each other than to the  $K_1$  response. The PV model predictions were similar across held-out conditions, while the LPV and NPV models scaled with exoskeleton torque. Full joint trajectories may be reproduced by rescaling and adding the average unperturbed gait cycle to the predictions. All comparisons used paired  $t$ -tests ( $\alpha = 0.05$ ) with a Holm-Sidak step-down correction for multiple comparisons.**

301

302

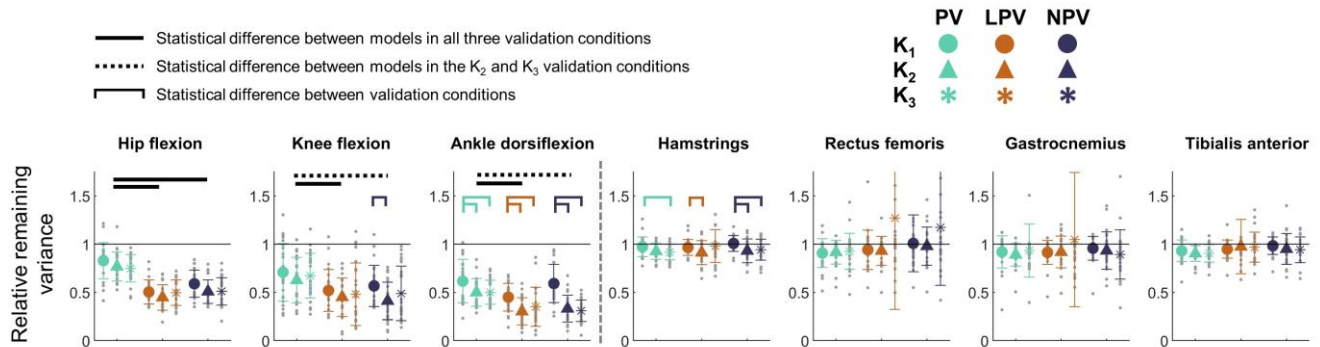


**Fig. 4. Average ( $\pm 1SD$ ) prediction accuracies for all participants and held-out conditions at a prediction horizon of 12.5% of a stride. Gray dots represent individual legs. Colored brackets denote statistically significant differences between held-out conditions for each model. Black horizontal bars denote significant differences between models across all three (solid) or two (dashed) held-out conditions. The large variance in the LPV model's predictions of rectus femoris and gastrocnemius responses in the held-out K<sub>3</sub> condition were due to bad predictions (RRV > 2) in a small number of legs. All comparisons used paired t-tests ( $\alpha = 0.05$ ) with a Holm-Sidak step-down correction for multiple comparisons.**

303

304 Predictions of myoelectric responses were poor (RRV  $\approx 1.00$ ) across all muscles and models, except at the  
305 shortest prediction horizon ( $\Delta = 6.25\%$ ). At the shortest prediction horizon, both the LPV and NPV models'  
306 predictions for the hamstrings, rectus femoris, and gastrocnemius were 10.7–15.0% more accurate than  
307 those of the PV model ( $p < 0.001$ ; Fig. 5).

308

309 Table II: Average ( $\pm$  1SD) RRV values for kinematic and myoelectric predictions at a 12.5% prediction  
 310 horizon.

Output	PV	LPV	NPV
Ankle angle <sup>†‡</sup>	$0.50 \pm 0.14$	$0.30 \pm 0.14$	$0.33 \pm 0.14$
Knee angle <sup>†‡</sup>	$0.62 \pm 0.24$	$0.45 \pm 0.20$	$0.41 \pm 0.19$
Hip angle <sup>†‡</sup>	$0.77 \pm 0.15$	$0.44 \pm 0.13$	$0.51 \pm 0.12$
Tibialis anterior	$0.90 \pm 0.08$	$0.97 \pm 0.28$	$0.95 \pm 0.15$
Soleus	$0.86 \pm 0.21$	$1.02 \pm 0.66$	$1.04 \pm 0.64$
Gastrocnemius	$0.89 \pm 0.12$	$0.91 \pm 0.16$	$0.93 \pm 0.19$
Vastus medialis	$0.92 \pm 0.12$	$0.93 \pm 0.15$	$0.98 \pm 0.20$
Rectus femoris	$0.87 \pm 0.21$	$0.91 \pm 0.38$	$0.94 \pm 0.42$
Lateral hamstrings	$0.93 \pm 0.08$	$0.91 \pm 0.13$	$0.93 \pm 0.12$
Gluteus medius	$0.95 \pm 0.08$	$0.96 \pm 0.10$	$0.98 \pm 0.10$

LPV = Linear phase-varying model; NPV = Nonlinear phase-varying model; PV = Phase-varying model

† Significant difference in prediction accuracy between the PV and LPV models

‡ Significant difference in prediction accuracy between the PV and NPV models

311

312

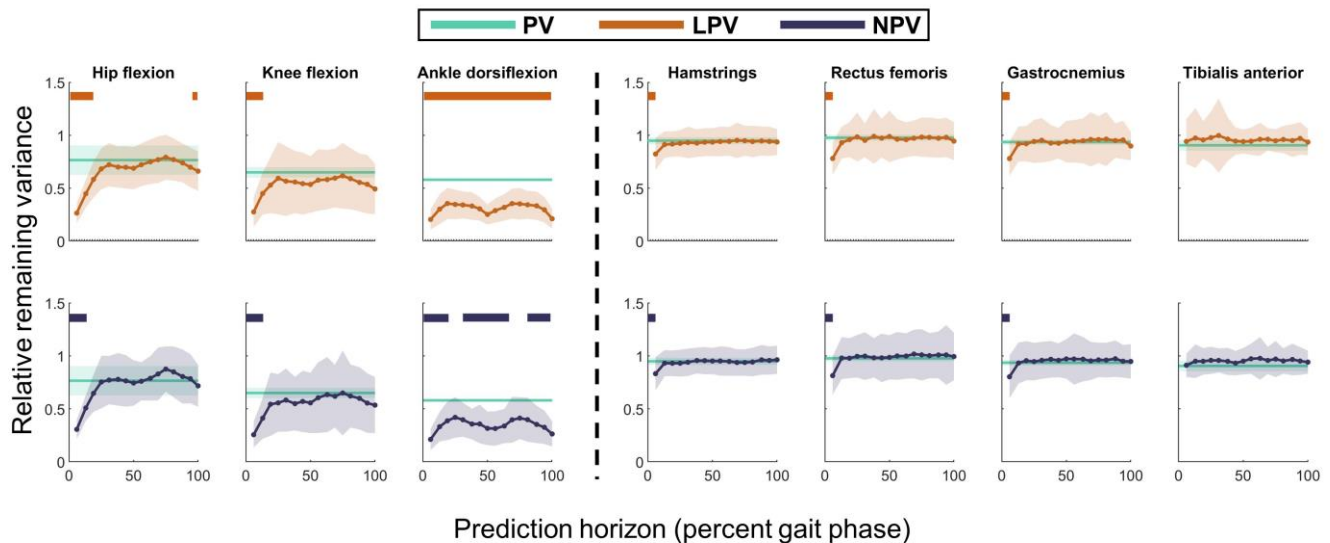


**Fig. 5. Prediction accuracy decreased with increasing prediction horizon. The PV model's predictions (green) were constant across prediction horizons. Horizontal bars denote predictions that were significantly more accurate than the PV model. The LPV (top; orange) and NPV (bottom; purple) models' prediction accuracies approached nearly constant values for prediction horizons beyond 25.0% of a stride for kinematic responses and 6.25% of a stride for myoelectric responses. The LPV and NPV models' predictions of ankle kinematics remained more accurate than PV model predictions across almost all prediction horizons, while knee and hip kinematic predictions were similar to those of the PV model beyond 25.0% of a stride.**

313



314 The LPV and NPV models' prediction accuracies improved with increasing training set size. As expected,  
315 the PV model's prediction accuracy was nearly constant across training set sizes ( $p > 0.005$ ; Fig. 6). For a  
316 prediction horizon of  $\Delta = 12.5\%$  of a stride, the LPV model's hip (RRV = 0.81) and knee (RRV = 0.78)  
317 prediction accuracies were significantly worse than  $RRV_{full}$  when using less than 50 strides of training data  
318 per exoskeleton condition ( $p < 0.001$ ). Similarly, the NPV model's hip and knee prediction accuracies  
319 approached  $RRV_{full}$  with approximately 50 strides of training data per condition ( $p < 0.001$ ). The LPV model  
320 required more data – up to 150 strides per condition – for prediction accuracies to approach  $RRV_{full}$  at the  
321 ankle, gastrocnemius, and tibialis anterior ( $p < 0.001$ ), though predictions were only 0.02–0.05 RRV points  
322 greater than  $RRV_{full}$  with 75 strides of training data per condition. The NPV model's myoelectric prediction  
323 accuracies approached  $RRV_{full}$ , in 25–75 strides of training data per condition ( $p < 0.001$ ; Fig. 6).

324

325

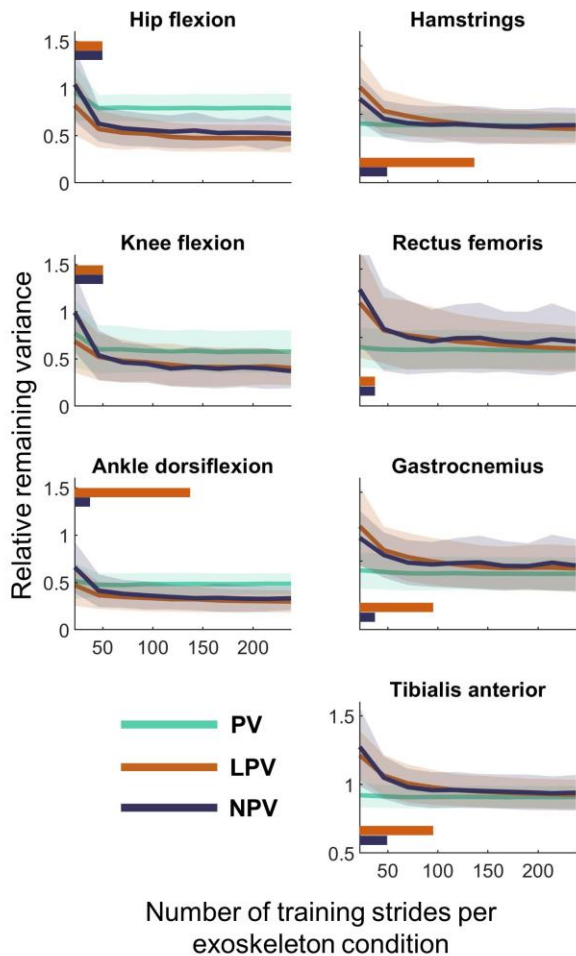


**Fig. 6.** Average ( $\pm 1SD$ ; shaded region) prediction accuracy of kinematic (left) and myoelectric (right) outputs for the PV (green), LPV (orange), and NPV (purple) models over training set sizes ranging from 24 to 240 cycles ( $RRV_{full}$ ). Prediction accuracies were reported at a 12.5% stride prediction horizon. Orange (LPV) and purple (NPV) horizontal bars denote the training set sizes that yielded significantly worse predictions than those of the full training set. The PV model's prediction accuracies were not significantly different from  $RRV_{full}$  at any training set size.

326

327 When validating on the held-out  $K_1$ ,  $K_2$ , and  $K_3$  conditions, the LPV and NPV model predictions reflected  
328 experimental changes in response between conditions (Fig. 3). For all models at a 12.5% stride prediction  
329 horizon, predictions of responses in the held-out  $K_1$  condition (interpolation) were 0.10–0.28 RRV points at  
330 the ankle and 0.04–0.09 points in the hamstrings less accurate than predictions of the  $K_2$  or  $K_3$  datasets ( $p <$   
331 0.001). Conversely, no statistical differences in prediction accuracies of the held-out  $K_2$  (interpolation) and  
332  $K_3$  (extrapolation) conditions were identified (Fig. 4). Improvements in kinematic prediction accuracy of the  
333 LPV model compared to the PV model were identified across the held-out  $K_1$ ,  $K_2$ , and  $K_3$  conditions ( $p <$   
334 0.001). Differences between the NPV and PV models' kinematic prediction accuracies in the held-out  $K_1$   
335 condition did not reach significance at the knee or ankle.

336 VI. DISCUSSION

337 We evaluated the ability of subject-specific phase-varying models to predict kinematic and myoelectric  
338 responses to ankle exoskeleton torques during treadmill walking. When predicting across three exoskeleton  
339 torque conditions, both linear and nonlinear models predicted kinematic responses to exoskeletons without  
340 knowledge of the specific user's physiological characteristics, supporting their potential utility as predictive  
341 tools for exoskeleton design and control. To our knowledge, this is the first study to predict kinematic and  
342 myoelectric responses to ankle exoskeletons using phase-varying models. Consistent with Floquet Theory  
343 and prior models of human locomotion, LPV models appear appropriate for predicting responses to  
344 exoskeleton torque over short prediction horizons, evidenced by its similar prediction accuracy to the more  
345 complex NPV model and improved prediction accuracy over the less complex PV model [25-27, 29].

346

347 The small and variable responses to exoskeleton torque exhibited by the unimpaired adults in this work  
348 highlight the challenge of altering kinematics with passive ankle exoskeletons. We found that even stiff  
349 exoskeletons ( $K_3 = 5.08 \text{ Nm/deg}$ ) only altered ankle kinematics on average by six degrees and integrated  
350 muscle activity by 14%. These small changes may correspond to larger changes in joint powers or metabolic  
351 demands and indicate that the present study is a rigorous test case [1, 2, 5, 24]. Despite small changes in gait,  
352 the LPV model's predictions explained more of the variance in kinematic responses to exoskeletons than the  
353 PV model, regardless of whether predictions interpolated ( $K_1$  and  $K_2$ ) or extrapolated ( $K_3$ ) relative to the  
354 training set. The LPV model's ability to predict kinematics within and slightly beyond the available training  
355 data supports its potential utility for predicting responses to untested exoskeleton designs or control laws.  
356 However, predictions of the held-out  $K_1$  condition highlight the importance of selecting experimental  
357 conditions that encode complex responses to torque.

358

359 Our hypothesis that the LPV model would predict kinematic and myoelectric responses more accurately than  
360 the PV model and as accurately as the NPV model was partially supported. The LPV model's kinematic and

361 myoelectric predictions were more accurate than those of the PV model only for prediction horizons less than  
362 18.75% and 6.25% of a stride, respectively, but the LPV and NPV models exhibited similar prediction  
363 accuracies across prediction horizons. The LPV and NPV models' similar predictions support research  
364 demonstrating that nonlinear spring-loaded inverted pendula (SLIPs) have similar predictive accuracy to  
365 linear models of human movement [25]. Compared to a nonlinear SLIP, the NPV model's feedforward neural  
366 network imposed fewer restrictions on model structure and enabling greater differences in prediction  
367 accuracy compared to a linear model. Therefore, the similarity of LPV and NPV model predictions supports  
368 the extension of Floquet Theory to gait with exoskeletons and indicates that, for rhythmic locomotion at a  
369 constant speed over level ground, linear phase-varying models have sufficiently complex structure to predict  
370 kinematic responses to exoskeletons [25-27, 29].

371

372 We observed comparable kinematic prediction accuracy to studies using physics-based and data-driven  
373 models of locomotion. Maus et al. evaluated multiple models' abilities to predict center-of-mass height  
374 during running and reported accuracies ranging from  $RRV \approx 0.15$  at a 15% prediction horizon to  $RRV \approx 0.85$   
375 beyond an 80% stride prediction horizon, for an exemplary participant [25]. Within a similar range of  
376 prediction horizons, the LPV model predicted kinematics across participants with average accuracies ranging  
377 from ( $0.30 < RRV < 0.45$ ) at a 12.5% prediction horizon and ( $0.34 < RRV < 0.77$ ) at an 81.3% prediction  
378 horizon. Similarly, Drnach et al. [43] used a hybrid linear model to predict response to functional electrical  
379 stimulation, reporting median RRV values (transformed from a fitness score) ranging from approximately  
380 0.11-1.04. However, the average unperturbed gait cycle was not subtracted from the data before computing  
381 the fitness score in [43]. The average unperturbed cycle accounts for a substantial portion of the variance in  
382 the perturbed signals, providing a less conservative prediction accuracy statistic than the RRV presented here.  
383 For example, if the unperturbed cycle had not been subtracted from the data in the present study, the LPV  
384 model's ankle predictions for one participant who exhibited large responses to torque would be  $RRV = 0.08$   
385 rather than the more conservative 0.21 reported. Comparable prediction accuracies to prior work indicate that

386 phase-varying models are potentially useful predictive tools for locomotion with ankle exoskeletons and may  
387 have similar predictive power to physics-based models of locomotion.

388

389 The convergence of LPV and NPV models' prediction accuracies to an approximately constant value at large  
390 prediction horizons (e.g.  $RRV_{LPV} \approx 0.70$  for knee kinematics at  $\Delta > 25.0\%$  of a stride) may be useful when  
391 selecting measurements for device design or control. The LPV and NPV models' kinematic prediction  
392 accuracies decreased rapidly from 6.25% to 18.75% stride prediction horizons, before reaching an  
393 approximately constant value. Ankle predictions remained better than those of the PV model across  
394 prediction horizons. Higher prediction accuracy at the ankle was unsurprising due to large responses to  
395 exoskeletons and the ankle's direct piecewise-linear relationship to passive exoskeleton torque. Since we  
396 trained on multiple exoskeleton conditions, the dynamics predicting future ankle kinematics are higher-  
397 dimensional than the simple exoskeleton torque-ankle angle relationship, suggesting that accurate predictions  
398 of ankle kinematics over large prediction horizons are likely for powered exoskeletons as well. Unlike the  
399 ankle, hip and knee kinematics were indirectly impacted by exoskeleton torque and their RRV values  
400 approached those of the PV model for prediction horizons above 18.75% of a stride. This result indicates that  
401 stride-specific initial posture and exoskeleton torque were predictive of indirect exoskeleton impacts on  
402 kinematics only for short prediction horizons. At large prediction horizons, measurements at an initial phase  
403 did not, on average, improve predictions of future posture. However, some participants' hip and knee  
404 kinematics were predicted up to 0.30 RRV points more accurately by the LPV and NPV models than the PV  
405 model across prediction horizons, suggesting that the prediction horizon at which stride-specific  
406 measurements no longer improve predicted responses to exoskeletons depends on the magnitude of the  
407 individual's response. The LPV and NPV models' accurate predictions over short prediction horizons make  
408 them primarily useful for exoskeleton control [10, 11]. For individuals that exhibit large responses to  
409 exoskeletons, however, LPV model-based predictions over stance may inform passive exoskeleton parameter  
410 selection. Guided adaptation and extended practice sessions [1, 17] or powered ankle exoskeletons [5, 6] may

411 elicit larger responses than those observed in this study and increase the maximum prediction horizons at  
412 which measurements at an initial posture improve predicted responses to torque, potentially expanding the  
413 settings in which model predictions are useful.

414

415 A major limitation of all three models was their inability to predict myoelectric responses. The LPV and NPV  
416 models predicted myoelectric signals more accurately than the PV model only for the shortest prediction  
417 horizon ( $\Delta = 6.25\%$ ). While exoskeleton torque and stiffness are known to impact average plantarflexor  
418 activity, we found that the average unperturbed gait cycle accounted for only 30-60% of the variance in the  
419  $K_2$  data, compared to 60-95% in kinematic signals [1, 9, 12]. Consequently, poor prediction accuracy may  
420 be partially attributed to small changes in muscle activity between the exoskeleton conditions. Alternatively,  
421 kinematic and myoelectric input variables may fail to encode nonlinear musculotendon dynamics, which are  
422 impacted by ankle exoskeletons, between the initial and final phases [21, 40]. Studies predicting muscle  
423 activity using physiologically-detailed models accounted for 60-99% of the variance in myoelectric signals,  
424 though they evaluated predictions on unperturbed walking conditions only [44, 45]. Still, the difference in  
425 prediction accuracy between the phase-varying models and physiologically-detailed models indicates that  
426 encoding musculotendon dynamics in the input variables is likely needed to improve myoelectric predictions  
427 for data-driven phase-varying models and represents an interesting area of future research.

428

429 Another limitation of subject-specific data-driven models, compared to physiologically-detailed models, is  
430 the amount of training data required to predict changes in gait with exoskeletons, which impacts models'  
431 utility in settings where minimizing data collection duration is critical to mitigating physical and logistical  
432 burdens on participants and families, such as in clinical gait laboratories. Improvements in prediction  
433 accuracy of the LPV and NPV models were small beyond 75–100 strides of training data per exoskeleton  
434 condition. The LPV model required more training data at the ankle, but a similar amount at the hip and knee  
435 to that used by Drnach et al., who trained a hybrid linear model using 45 seconds of data across two

436 experimental conditions [43]. For unimpaired, steady-state locomotion, data-driven linear models appear to  
437 require 75–125 strides of training data per condition, which supports their feasibility only in gait analysis  
438 settings with treadmills or long walkways [6, 7]. Additional dimensionality reduction, such as via sparse  
439 regression, may reduce the LPV model’s complexity and demand for training data [25, 31, 46]. However,  
440 when only one training condition or a few strides are collected, as is standard in clinical gait analysis, phase-  
441 varying model predictions will be poor and physiologically-detailed or population-specific models may  
442 generate more accurate predictions [8, 19, 44, 45].

443

444 Subject-specific data-driven phase-varying models of gait with exoskeletons have benefits and limitations  
445 compared to predictive musculoskeletal models. While we investigated only a specific subset of phase-  
446 varying models, we showed that this class of model can predict kinematic responses to exoskeletons without  
447 detailed knowledge of the physiological and neuromuscular factors influencing responses to exoskeletons.  
448 Conversely, uncertainty in the mechanisms driving complex responses to exoskeletons may limit  
449 physiologically-detailed models’ accuracy [13, 24]. While predictive musculoskeletal models may generate  
450 “what-if” predictions without experimental data, data may be needed to specify initial postures and tune  
451 subject-specific parameters. Phase-varying models can similarly perform subject-specific “what-if”  
452 predictions when application-specific training data are available. Unlike physiologically-detail models, this  
453 and prior work exemplify phase-varying models’ ability to take arbitrary measurements as inputs, enabling  
454 their application using a range of experimental resources [25, 26, 31]. Extending data-driven predictions to  
455 “what-if” scenarios and improving predicted myoelectric responses to exoskeletons, combined with  
456 analytical tools for phase-varying systems(e.g. [31]), may facilitate prediction and analysis of individualized  
457 exoskeleton impacts on gait mechanics and motor control.

458

459 VII. CONCLUSION

460 To our knowledge, this is the first study to predict subject-specific responses to ankle exoskeletons using  
461 phase-varying models. Without making assumptions about individual physiology or motor control, an LPV  
462 model predicted short-time kinematic responses to bilateral passive ankle exoskeletons, though predicting  
463 myoelectric responses remains challenging. Results support the utility of LPV models for studying and  
464 predicting response to exoskeleton torque. Improving data-driven models and experimental protocols to study  
465 and predict myoelectric responses to exoskeletons represents an important direction for future research.  
466 Modeling responses to exoskeletons or other assistive devices using a phase-varying perspective has the  
467 potential to inform exoskeleton design for a range of user groups.

468



469 VIII. AUTHOR CONTRIBUTIONS

470  
471 MCR was involved in the conception and design of the study, carried out exoskeleton design and fabrication,  
472 data collection, data preprocessing, statistical analyses and data interpretation, and drafted the manuscript.  
473 BSB was involved in the conception and design of the study and carried out model development and coding,  
474 contributed to the initial manuscript draft, and critically revised the manuscript. SAB critically revised the  
475 manuscript and acquired funding for this work and was involved in the conception and design of the study,  
476 model development, and data interpretation. KMS critically revised the manuscript, acquired funding for this  
477 work, and was involved in the conception and design of the study and data interpretation.

478

479 IX. DATA ACCESSIBILITY

480 All experimental datasets and code using in this study are freely available and can be accessed on  
481 <https://simtk.org/projects/ankleexopred>.

482

483 X. ETHICS

484 This study was approved by the University of Washington Institutional Review Board #47744. All research  
485 participants provided informed consent prior to participating in the study, obtained by MCR.

486

487 XI. FUNDING STATEMENT

488 This material is based upon work supported by the U. S. Army Research Office under grant number W911NF-  
489 16-1-0158 to SAB, the National Science Foundation under grant No. CBET-1452646 to KMS, the National  
490 Science Foundation Graduate Research Fellowship Program under Grant No. DGE-1762114 to MCR, and  
491 the AMP Center Strategic Research Initiative of the University of Washington College of Engineering.

492

493 XII. REFERENCES

- 494 [1] Collins, S.H., Wiggin, M.B. & Sawicki, G.S. 2015 Reducing the energy cost of human walking using an  
495 unpowered exoskeleton. *Nature* **522**, 212-215.
- 496 [2] Kerkum, Y.L., Buizer, A.I., van den Noort, J.C., Becher, J.G., Harlaar, J. & Brehm, M.-A. 2015 The  
497 effects of varying ankle foot orthosis stiffness on gait in children with spastic cerebral palsy who walk with  
498 excessive knee flexion. *PloS one* **10**, e0142878.
- 499 [3] Owen, E. 2010 The importance of being earnest about shank and thigh kinematics especially when using  
500 ankle-foot orthoses. *Prosthetics and orthotics international* **34**, 254-269.
- 501 [4] Lerner, Z.F., Harvey, T.A. & Lawson, J.L. 2019 A Battery-Powered Ankle Exoskeleton Improves Gait  
502 Mechanics in a Feasibility Study of Individuals with Cerebral Palsy. *Annals of biomedical engineering* **47**,  
503 1345-1356.
- 504 [5] Mooney, L.M. & Herr, H.M. 2016 Biomechanical walking mechanisms underlying the metabolic  
505 reduction caused by an autonomous exoskeleton. *Journal of neuroengineering and rehabilitation* **13**, 4.
- 506 [6] Zhang, J., Fiers, P., Witte, K.A., Jackson, R.W., Poggensee, K.L., Atkeson, C.G. & Collins, S.H. 2017  
507 Human-in-the-loop optimization of exoskeleton assistance during walking. *Science* **356**, 1280-1284.
- 508 [7] Ding, Y., Kim, M., Kuindersma, S. & Walsh, C.J. 2018 Human-in-the-loop optimization of hip assistance  
509 with a soft exosuit during walking. *Science Robotics* **3**, eaar5438.
- 510 [8] Ries, A.J., Novacheck, T.F. & Schwartz, M.H. 2014 A data driven model for optimal orthosis selection  
511 in children with cerebral palsy. *Gait & posture* **40**, 539-544.
- 512 [9] Steele, K.M., Jackson, R.W., Shuman, B.R. & Collins, S.H. 2017 Muscle recruitment and coordination  
513 with an ankle exoskeleton. *Journal of biomechanics* **59**, 50-58.
- 514 [10] Åström, K.J. & Murray, R.M. 2010 *Feedback systems: an introduction for scientists and engineers*,  
515 Princeton university press.

- 516 [11] Koller, J.R., Jacobs, D.A., Ferris, D.P. & Remy, C.D. 2015 Learning to walk with an adaptive gain  
517 proportional myoelectric controller for a robotic ankle exoskeleton. *Journal of neuroengineering and*  
518 *rehabilitation* **12**, 97.
- 519 [12] Jackson, R.W. & Collins, S.H. 2015 An experimental comparison of the relative benefits of work and  
520 torque assistance in ankle exoskeletons. *Journal of Applied Physiology* **119**, 541-557.
- 521 [13] Ries, A.J., Novacheck, T.F. & Schwartz, M.H. 2015 The efficacy of ankle-foot orthoses on improving  
522 the gait of children with diplegic cerebral palsy: a multiple outcome analysis. *PM&R* **7**, 922-929.
- 523 [14] Bregman, D., Van der Krogt, M., De Groot, V., Harlaar, J., Wisse, M. & Collins, S. 2011 The effect of  
524 ankle foot orthosis stiffness on the energy cost of walking: a simulation study. *Clinical Biomechanics* **26**,  
525 955-961.
- 526 [15] Rosenberg, M. & Steele, K.M. 2017 Simulated impacts of ankle foot orthoses on muscle demand and  
527 recruitment in typically-developing children and children with cerebral palsy and crouch gait. *PLoS one* **12**,  
528 e0180219.
- 529 [16] Uchida, T.K., Seth, A., Pouya, S., Dembia, C.L., Hicks, J.L. & Delp, S.L. 2016 Simulating Ideal  
530 Assistive Devices to Reduce the Metabolic Cost of Running. *PLoS one* **11**, e0163417.
- 531 [17] Selinger, J.C., Wong, J.D., Simha, S.N. & Donelan, J.M. 2019 How humans initiate energy optimization  
532 and converge on their optimal gaits. *Journal of Experimental Biology* **222**, jeb198234.
- 533 [18] Delp, S.L., Anderson, F.C., Arnold, A.S., Loan, P., Habib, A., John, C.T., Guendelman, E. & Thelen,  
534 D.G. 2007 OpenSim: open-source software to create and analyze dynamic simulations of movement. *IEEE*  
535 *transactions on biomedical engineering* **54**, 1940-1950.
- 536 [19] Pitto, L., Kainz, H., Falisse, A., Wesseling, M., Van Rossom, S., Hoang, H., Papageorgiou, E.,  
537 Hallemans, A., Desloovere, K. & Molenaers, G. 2019 SimCP: a simulation platform to predict gait  
538 performance following orthopedic intervention in children with Cerebral Palsy. *Frontiers in neurorobotics*  
539 **13**, 54.

- 540 [20] Handsfield, G.G., Meyer, C.H., Abel, M.F. & Blemker, S.S. 2016 Heterogeneity of muscle sizes in the  
541 lower limbs of children with cerebral palsy. *Muscle & nerve* **53**, 933-945.
- 542 [21] Sawicki, G.S. & Khan, N.S. 2016 A Simple Model to Estimate Plantarflexor Muscle–Tendon Mechanics  
543 and Energetics During Walking With Elastic Ankle Exoskeletons. *IEEE Transactions on Biomedical*  
544 *Engineering* **63**, 914-923.
- 545 [22] Steele, K.M., Rozumalski, A. & Schwartz, M.H. 2015 Muscle synergies and complexity of  
546 neuromuscular control during gait in cerebral palsy. *Developmental Medicine & Child Neurology* **57**, 1176-  
547 1182.
- 548 [23] Chisholm, A.E. & Perry, S.D. 2012 Ankle-foot orthotic management in neuromuscular disorders:  
549 recommendations for future research. *Disability and Rehabilitation: Assistive Technology* **7**, 437-449.
- 550 [24] Jackson, R.W., Dembia, C.L., Delp, S.L. & Collins, S.H. 2017 Muscle–tendon mechanics explain  
551 unexpected effects of exoskeleton assistance on metabolic rate during walking. *Journal of Experimental*  
552 *Biology* **220**, 2082-2095.
- 553 [25] Maus, H.-M., Revzen, S., Guckenheimer, J., Ludwig, C., Reger, J. & Seyfarth, A. 2015 Constructing  
554 predictive models of human running. *Journal of The Royal Society Interface* **12**, 20140899.
- 555 [26] Wang, Y. & Srinivasan, M. System identification and stability analyses of steady human locomotion.  
556 *Foot* **300**, 600.
- 557 [27] Hartman, P. 2002 *Ordinary differential equations*. 2nd ed. ed. Philadelphia, Philadelphia : Society for  
558 Industrial and Applied Mathematics.
- 559 [28] Burden, S.A., Revzen, S. & Sastry, S.S. 2015 Model reduction near periodic orbits of hybrid dynamical  
560 systems. *IEEE Transactions on Automatic Control* **60**, 2626-2639.
- 561 [29] Ankaralı, M.M., Sefati, S., Madhav, M.S., Long, A., Bastian, A.J. & Cowan, N.J. 2015 Walking  
562 dynamics are symmetric (enough). *Journal of the Royal Society Interface* **12**, 20150209.
- 563 [30] Revzen, S. & Guckenheimer, J.M. 2008 Estimating the phase of synchronized oscillators. *Physical*  
564 *Review E* **78**, 051907.

- 565 [31] Revzen, S. & Guckenheimer, J.M. 2011 Finding the dimension of slow dynamics in a rhythmic system.  
566 *Journal of The Royal Society Interface* **9**, 957-971.
- 567 [32] Kadaba, M.P., Ramakrishnan, H. & Wootten, M. 1990 Measurement of lower extremity kinematics  
568 during level walking. *Journal of orthopaedic research* **8**, 383-392.
- 569 [33] Hermens, H.J., Freriks, B., Merletti, R., Stegeman, D., Blok, J., Rau, G., Disselhorst-Klug, C. & Hägg,  
570 G. 1999 European recommendations for surface electromyography. *Roessingh research and development* **8**,  
571 13-54.
- 572 [34] Rajagopal, A., Dembia, C.L., DeMers, M.S., Delp, D.D., Hicks, J.L. & Delp, S.L. 2016 Full-body  
573 musculoskeletal model for muscle-driven simulation of human gait. *IEEE transactions on biomedical*  
574 *engineering* **63**, 2068-2079.
- 575 [35] Villarreal, D.J., Poonawala, H.A. & Gregg, R.D. 2016 A robust parameterization of human gait patterns  
576 across phase-shifting perturbations. *IEEE Transactions on Neural Systems and Rehabilitation Engineering*  
577 **25**, 265-278.
- 578 [36] Revzen, S. 2020 BIRDS Lab mathmisc. (GitHub).
- 579 [37] Glorot, X. & Bengio, Y. 2010 Understanding the difficulty of training deep feedforward neural networks.  
580 In *Proceedings of the thirteenth international conference on artificial intelligence and statistics* (pp. 249-  
581 256).
- 582 [38] LeCun, Y., Bengio, Y. & Hinton, G. 2015 Deep learning. *nature* **521**, 436-444.
- 583 [39] Zajac, F.E., Neptune, R.R. & Kautz, S.A. 2002 Biomechanics and muscle coordination of human  
584 walking: Part I: Introduction to concepts, power transfer, dynamics and simulations. *Gait & posture* **16**, 215-  
585 232.
- 586 [40] Zajac, F.E. 1989 Muscle and tendon: properties, models, scaling, and application to biomechanics and  
587 motor control. *Critical reviews in biomedical engineering* **17**, 359-411.
- 588 [41] Carter, G.C. 1987 Coherence and time delay estimation. *Proceedings of the IEEE* **75**, 236-255.
- 589 [42] Glantz, S. 2012 *Primer of Biostatistics*, 7th edn, pp. 65–67. (New York: McGraw-Hill).

- 590 [43] Drnach, L., Allen, J.L., Essa, I. & Ting, L.H. 2019 A Data-Driven Predictive Model of Individual-  
591 Specific Effects of FES on Human Gait Dynamics. In *2019 International Conference on Robotics and  
592 Automation (ICRA)* (pp. 5090-5096, IEEE).
- 593 [44] Geyer, H., Seyfarth, A. & Blickhan, R. 2006 Compliant leg behaviour explains basic dynamics of  
594 walking and running. *Proceedings of the Royal Society B: Biological Sciences* **273**, 2861-2867.
- 595 [45] Martelli, S., Calvetti, D., Somersalo, E. & Viceconti, M. 2015 Stochastic modelling of muscle  
596 recruitment during activity. *Interface focus* **5**, 20140094.
- 597 [46] Brunton, S.L., Proctor, J.L. & Kutz, J.N. 2016 Discovering governing equations from data by sparse  
598 identification of nonlinear dynamical systems. *Proceedings of the National Academy of Sciences* **113**, 3932-  
599 3937.
- 600